Journal of Geothermal Research and Volcanology (2026) 76-89

Contents lists available at FoundAE

Journal of Geothermal Research and Volcanology

Journal homepage: https://ejournal.foundae.com/index.php/jograv/index

Stable terrain clusters, limited lithological discrimination: Evaluating DEM-based morphometric classification in an eroded paleo-volcanic landscape

Rizqi Prastowo[a,*], Ignatius Adi Prabowo[b]

[a] Department of Mining Engineering, Faculty of Engineering and Planning, Institut Teknologi Nasional Yogyakarta, Sleman, Yogyakarta 55281, Indonesia
[b] Faculty of Built Environment and Surveying, Universiti Teknologi Malaysia, Johor Bahru, Johor 81310, Malaysia

ARTICLE INFO

Keywords:
Digital elevation model (DEM);
Terrain classification;
Unsupervised clustering;
Lithological discrimination;
Eroded volcanic landscapes.

ABSTRACT

Morphometric classification of digital elevation models (DEMs) offers a potential approach to characterizing deeply eroded volcanic landscapes where original volcanic edifices and lithological boundaries are obscured by long-term denudation. However, the extent to which statistically stable terrain clusters correspond to geological units remains insufficiently understood. This study evaluates the geomorphological and lithological significance of unsupervised terrain classification in the eroded paleovolcanic complex of the Kulon Progo Mountains, Indonesia. Eight morphometric attributes derived from the Indonesian National Digital Elevation Model (DEMNAS; approximately 8 m spatial resolution) were aggregated into 26,372 analysis cells at 120 m resolution, standardized, transformed using principal component analysis, and classified using K-means clustering. Cluster selection, reproducibility, and geological correspondence were evaluated using internal clustering indices, conventional and spatial block bootstrapping, geological agreement metrics, and comparisons with single-attribute classifications. Four terrain clusters were identified, representing relatively weakly dissected upper surfaces, deeply incised valley slopes, transitional footslopes, and low-relief alluvial plains and Sentolo hills. The classification exhibited high reproducibility under cell-based bootstrapping (adjusted Rand index, ARI = 0.968) and spatial block bootstrapping (ARI = 0.878). Nevertheless, agreement with the regional geological map was moderate (Cramér's V = 0.454) and lower than that obtained from slope-only (0.511) and relief-only (0.551) classifications. Furthermore, mapped andesite intrusions and the Kebobutak Formation exhibited weak morphometric separability (|Cliff's δ| ≤ 0.27 across individual attributes). These findings demonstrate that stable multivariate terrain partitions do not necessarily improve lithological discrimination. DEM-based morphometric clustering primarily captures landscape position and erosional dissection in this setting, highlighting the need for independent geological validation and complementary subsurface observations when interpreting terrain clusters as lithological boundaries.

1. Introduction

Digital elevation models (DEMs) have become fundamental resources for quantitative geomorphological analysis, providing spatially continuous representations of terrain morphology and enabling systematic investigation of landscape organization, topographic variability, and surface processes. Advances in the availability and resolution of elevation datasets have facilitated the development of automated methods for identifying landforms, characterizing terrain complexity, and investigating geomorphological relationships with geological structures. In volcanic environments, DEM-derived morphometric parameters have been extensively employed to characterize volcanic edifices, quantify morphological variations, and reconstruct aspects of volcanic landscape evolution. Systematic morphometric analysis provides an objective framework for examining volcanic morphology through measurable characteristics such as slope, relief, surface geometry, and edifice configuration [1, 2]. However, conventional volcanic morphometry often assumes that the principal boundaries and geometric characteristics of volcanic edifices remain sufficiently preserved for quantitative interpretation. This assumption becomes increasingly problematic in ancient volcanic landscapes where prolonged erosion, tectonic deformation, and weathering have substantially modified or removed the original volcanic topography.

* Corresponding author.
E-mail address: rizqi@itny.ac.id (R. Prastowo).

https://doi.org/10.58524/jograv.v1i2.193
Received 15 June 2026; Received in revised form 28 July 2026; Accepted 28 September 2026
Available online 30 September 2026
3163-3471/Published by FoundAE (Foundation of Advanced Education).

Deeply eroded volcanic terrains present particular challenges for geological interpretation because contemporary landforms reflect the combined effects of original volcanic construction, subsequent tectonic processes, differential weathering, and long-term denudation. Progressive erosion may remove volcanic summits, expose deeper volcanic structures, modify drainage organization, and redistribute topographic contrasts across different geological units. DEM-based investigations of degraded volcanic landscapes have demonstrated that erosional processes can significantly modify volcanic morphology and obscure the original architectural characteristics of volcanic edifices [3–5]. Furthermore, the relationship between topographic expression and bedrock lithology is not necessarily unique. Differences in rock mass strength, fracture characteristics, and resistance to weathering may influence landscape evolution, but similar morphologies can develop in different geological materials under comparable environmental conditions [6, 7]. Conversely, substantial geomorphological variability may occur within the same lithological formation because of differences in terrain position, drainage development, and erosion intensity. Consequently, the interpretation of present-day terrain characteristics as direct indicators of lithological boundaries requires careful evaluation, particularly in tropical volcanic regions characterized by prolonged weathering and extensive landscape dissection [8–10].

Automated terrain classification offers an alternative approach for characterizing geomorphological organization without requiring the reconstruction of original volcanic edifice boundaries. By grouping spatial observations according to similarities in measurable terrain attributes, unsupervised classification can identify recurring morphological patterns and delineate terrain domains across heterogeneous landscapes. Iwahashi and Pike [4] developed an automated classification framework based on slope gradient, local convexity, and surface texture, demonstrating that geometric terrain characteristics can be combined to produce reproducible geomorphological classifications. Subsequent developments have extended these approaches to large spatial datasets using segmentation and clustering algorithms. Global terrain classification based on DEM-derived attributes has demonstrated the usefulness of K-means clustering for recognizing broad geomorphological patterns and comparing terrain classes with geological and geomorphological information [3, 11]. Nevertheless, the statistical grouping of topographically similar cells does not necessarily imply geological equivalence. Terrain classes are initially defined by similarity in morphometric feature space, and their interpretation as geological or lithological units requires independent validation.

The integration of multiple morphometric attributes is commonly intended to capture complementary aspects of landscape morphology that cannot be represented adequately by a single terrain descriptor. Slope and local relief characterize terrain steepness and elevation variability, whereas terrain ruggedness and curvature provide information about surface complexity and the spatial arrangement of ridges and valleys. Drainage density can characterize aspects of landscape dissection, while hypsometric properties and topographic position may reflect variations in relative elevation and geomorphological setting. Combining these variables can potentially improve discrimination among terrain domains with contrasting erosional characteristics. However, increasing the number of morphometric attributes does not necessarily improve the ability to distinguish geological units. Strong correlations among terrain variables, differences in the spatial scales over which attributes are calculated, and sensitivity to DEM-derived artifacts may cause multivariate classifications to emphasize geomorphological variation unrelated to lithological boundaries. Therefore, the effectiveness of multi-attribute classification should be evaluated against simpler alternatives rather than assuming that additional variables automatically improve geological discrimination.

K-means clustering provides a computationally efficient framework for partitioning continuous morphometric observations according to their similarity in multidimensional feature space. Its application is particularly relevant to exploratory terrain analysis because it does not require predefined geological labels during classification. Nevertheless, the resulting partition depends on several methodological decisions, including attribute selection, data transformation, feature scaling, dimensionality reduction, cluster initialization, and the specified number of clusters. A comprehensive evaluation of clustering methods has emphasized that algorithmic performance should be interpreted in relation to the characteristics of the underlying dataset and the objectives of the classification [6]. Principal component analysis (PCA) can reduce redundancy among correlated terrain attributes by transforming the original variables into orthogonal components that represent major directions of data variance [7]. However, the preservation of statistical variance does not guarantee the preservation of features most relevant to lithological differentiation. Consequently, a multivariate terrain classification may generate internally coherent clusters without necessarily improving correspondence with independently mapped geological formations [12, 13].

A critical methodological challenge is the distinction between clustering reproducibility and geological validity. Internal validation metrics, including the silhouette coefficient and Davies–Bouldin index, quantify different aspects of cluster compactness and separation within the selected feature space [8,9]. Resampling approaches can additionally evaluate whether similar clusters are recovered under changes in data sampling or initialization. However, high internal consistency and numerical stability do not demonstrate that the resulting clusters represent distinct lithological units. Geological validity requires external comparison against independent geological information, such as mapped formations, field observations, petrological characteristics, or complementary geophysical datasets. This distinction becomes particularly important in gridded terrain analysis because neighboring cells exhibit substantial spatial dependence. Conventional random resampling may overestimate the robustness of a spatial classification by repeatedly sampling observations that share similar terrain characteristics. Spatially structured resampling provides a more cautious approach to evaluating model behavior in geographically dependent datasets [6, 14, 15]. Therefore, assessments of automated terrain classification should distinguish among internal clustering quality, spatial reproducibility, and agreement with independently established geological boundaries.

The interpretation of DEM-derived terrain classes presents additional challenges in densely vegetated tropical landscapes, where bedrock exposures may be obscured by vegetation, thick weathering profiles, and soil cover. Previous investigations have demonstrated that integrating remotely sensed spectral information with high-resolution topographic data can improve lithological characterization in vegetated terrain [11]. However, topographic information alone cannot always resolve boundaries between geological units with similar surface expressions. In Indonesia, the Indonesian National Digital Elevation Model (DEMNAS) provides elevation data at approximately 0.27 arcsecond spatial resolution, corresponding to roughly 8 m in the study region. DEMNAS offers opportunities for detailed quantitative terrain analysis, although the interpretation of derived morphometric attributes must consider the effects of vegetation, surface representation, interpolation, and elevation uncertainty. Previous assessments have raised questions regarding the extent to which DEMNAS represents the bare-earth

terrain surface rather than surface features associated with vegetation and other objects [4, 16]. Such uncertainties may influence local roughness, curvature, drainage extraction, and other terrain attributes, particularly where morphometric contrasts between adjacent geological units are subtle.

The Kulon Progo Mountains of southern Java, Indonesia, provide a suitable geological setting for evaluating these challenges. The region comprises an ancient volcanic complex developed during the Oligocene–Miocene and subsequently modified by tectonic deformation, uplift, weathering, and prolonged erosion [13,14]. Its present-day morphology consists of dissected volcanic uplands, incised valleys, transitional hillslopes, and surrounding lower-relief terrain. Geological mapping identifies extensive volcanic rock assemblages, andesitic intrusive bodies, carbonate formations, and younger alluvial deposits [15]. The distribution of these units provides a reference framework for evaluating the relationship between geomorphological patterns and geological boundaries. However, the strongly eroded character of the volcanic landscape complicates lithological interpretation because intrusive and extrusive volcanic rocks may develop overlapping terrain characteristics, whereas different geomorphological domains may occur within the same volcanic formation. The coexistence of distinct erosional landforms and heterogeneous geological materials makes Kulon Progo a relevant natural setting for investigating the geological significance of unsupervised morphometric classification.

Despite substantial progress in DEM-based geomorphometry and automated terrain classification, the relationship between statistically stable morphometric clusters and their capacity to discriminate lithological units remains an important issue in deeply eroded volcanic landscapes. Previous studies have demonstrated the usefulness of terrain classification for characterizing landform patterns, but the geological interpretation of such classifications requires separate evaluation. In particular, it remains necessary to determine whether combining multiple terrain attributes improves geological correspondence relative to simpler classifications based on slope or relief alone. It is equally important to assess whether numerical clustering stability persists under spatially structured resampling and whether lithologically distinct but morphologically similar volcanic and intrusive rocks can be reliably differentiated. These questions are relevant to the interpretation of unsupervised classifications because the stability of a terrain partition may reflect persistent geomorphological organization rather than the spatial distribution of individual geological formations.

This study evaluates the relationship between morphometric cluster stability and lithological discrimination within the deeply eroded paleovolcanic landscape of the Kulon Progo Mountains. Eight terrain attributes derived from DEMNAS are integrated using PCA and K-means clustering to characterize geomorphological variability across a 20 × 20 km study area. The investigation addresses four specific objectives: (1) to identify and characterize morphometric terrain domains associated with variations in topographic position, surface complexity, and landscape dissection; (2) to evaluate cluster reproducibility through repeated initialization, conventional bootstrap resampling, and spatial block bootstrap; (3) to quantify the correspondence between multivariate terrain classifications and regional geological formations using external agreement metrics and comparisons with slope-only and relief-only clustering; and (4) to examine the morphometric separability of mapped andesitic intrusions and surrounding volcanic formations. The central hypothesis is that multivariate terrain classification can reveal geomorphological differentiation without necessarily improving lithological discrimination. By explicitly separating numerical reproducibility from geological correspondence, this study seeks to establish a more rigorous interpretive framework for assessing the capabilities and limitations of DEM-based unsupervised terrain classification in strongly eroded volcanic environments.

2. Method

2.1. Study area and geological setting

The study was conducted in the central and southern Kulon Progo Mountains, Special Region of Yogyakarta, Indonesia, within a 20 × 20 km study window extending from 390,000 to 410,000 m E and 9,130,000 to 9,150,000 m N in the WGS 84/UTM Zone 49S coordinate system (Fig. 1). The study area encompasses the deeply eroded paleovolcanic terrain associated with the Gajah and Ijo volcanic complexes, together with adjacent lower-relief landscapes. The region is characterized by substantial topographic variability, including dissected volcanic uplands, incised valleys, transitional hillslopes, carbonate hills, and surrounding alluvial plains.

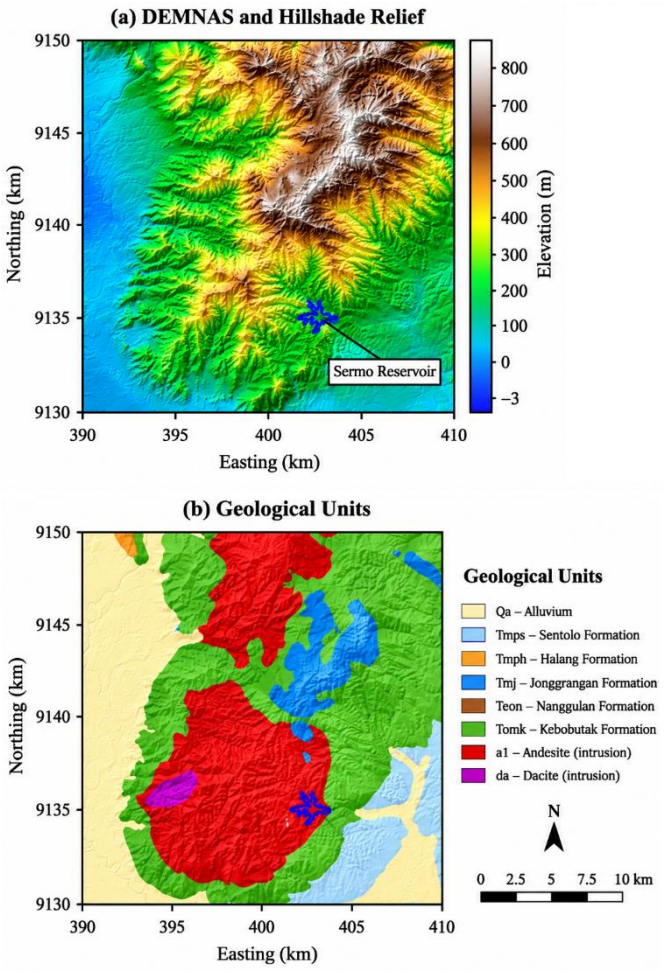


Fig. 1. Study area in the Kulon Progo Mountains, Indonesia: (a) DEMNAS-derived elevation model and (b) regional geological units obtained from the digital geological map [16]. The blue outline indicates the Sermo Reservoir.

The regional geological framework was established using the Geological Map of the Yogyakarta Quadrangle [15] and the digital geological dataset distributed by the Geological Research and Development Centre [16]. The principal mapped lithological units comprise the Kebobutak Formation (Tomk), andesitic intrusions (a1), Quaternary alluvium (Qa), the Sentolo Formation (Tmps), and the Jonggrangan Formation (Tmj). These units represent approximately 37.1%, 26.0%, 23.2%, 7.3%, and 5.1% of the

mapped study area, respectively. Minor units, including dacitic intrusions, the Halang Formation, and the Nanggulan Formation, individually account for less than 1% of the area.

The geological diversity and strongly dissected topography provide a suitable setting for evaluating whether morphometric similarities correspond to lithological relationships or primarily reflect landscape position and erosional modification. In particular, the spatial association between the Kebobutak Formation and andesitic intrusive bodies provides a geological test case for assessing the capacity of terrain attributes to distinguish mapped volcanic and intrusive rock units.

Fig. 1 presents the DEMNAS-derived elevation distribution and the corresponding geological units within the study window. The geological map was used as an external reference for evaluating the resulting terrain classifications rather than as an input to the unsupervised clustering procedure. This separation was essential to ensure that the clustering algorithm identified terrain patterns independently of the geological labels subsequently used for interpretation.

2.2. *Digital elevation and geological data preparation*

The primary elevation dataset was obtained from the Indonesian National Digital Elevation Model (DEMNAS), using tiles 1408-21 and 1408-23. The source data have a spatial resolution of approximately 0.27 arcseconds, equivalent to approximately 8 m in the study region. The original DEM tiles, referenced in geographic coordinates, were mosaicked and reprojected into WGS 84/UTM Zone 49S. Bilinear interpolation was applied during reprojection to obtain a continuous elevation raster with an 8 m grid spacing.

The reprojected DEM was subsequently clipped to the predefined 20 × 20 km study window. Elevation values within the resulting dataset ranged from approximately −3 to 842 m. The preprocessing procedure was designed to maintain a consistent projected grid for subsequent terrain analysis and spatial comparison with geological information.

The surface of the Sermo Reservoir was excluded from terrain attribute computation because water-surface elevation does not represent the underlying bedrock topography. The reservoir mask was constructed by identifying spatially connected low-gradient cells, defined by a slope threshold below 0.5°, at an elevation of approximately 130.9 m. The resulting masked reservoir area covered approximately 0.84 km². This exclusion reduced the influence of artificially uniform water-surface elevations on terrain derivatives and the subsequent classification.

The geological reference dataset was prepared from the digital geological polygons corresponding to the regional geological map [16]. The original polygons were rasterized onto an approximately 4 m geographic grid and subsequently resampled to the 8 m DEM grid using nearest-neighbor interpolation. This approach preserved categorical geological labels during resampling and enabled spatial comparison between geological formations and DEM-derived morphometric attributes.

Geological labels were retained exclusively for external evaluation and post-classification interpretation. They were not incorporated into PCA, K-means training, or cluster-number selection. The analysis was implemented in Python using NumPy, SciPy, scikit-image, rasterio, and scikit-learn [17]. These packages supported raster preprocessing, terrain attribute extraction, numerical transformation, multivariate analysis, clustering, and evaluation of classification results [17, 18].

2.3. *Extraction of morphometric terrain attributes*

Eight DEM-derived morphometric attributes were selected to characterize complementary aspects of terrain steepness, surface complexity, landscape dissection, and relative topographic position. The selected attributes comprised mean slope, slope variability, local relief, vector ruggedness measure (VRM), profile curvature variability, drainage density, local hypsometric integral, and regional topographic position index (TPI).

Slope gradient was calculated using the Horn finite-difference operator [18], whereas profile curvature was derived using the Zevenbergen–Thorne polynomial approach [19]. Before curvature computation, the DEM was smoothed using a Gaussian filter with a standard deviation of 1.5 pixels to reduce high-frequency elevation variability.

Mean slope, slope standard deviation, local relief, and curvature variability were subsequently calculated using 500 m moving windows. These neighborhood-scale descriptors were intended to characterize the texture of terrain units rather than only the instantaneous morphology of individual raster cells.

Local relief was defined as the difference between the maximum and minimum elevations within the specified neighborhood. Slope variability was represented by the standard deviation of slope angles, while curvature variability was expressed as the standard deviation of profile curvature. Together, these attributes characterized differences in terrain steepness, topographic amplitude, and the frequency of transitions between convex and concave surface forms.

Terrain ruggedness was quantified using the vector ruggedness measure developed by Sappington et al. [20]. VRM evaluates variability in the orientation of surface-normal vectors and provides a measure of three-dimensional terrain complexity. VRM was calculated as:

$$VRM = 1 - |\Sigma n_i| / n \quad \ldots (1)$$

where n_i represents the unit normal vector of each DEM cell and n is the number of cells within the calculation neighborhood. Local VRM was initially calculated using a 5 × 5 pixel neighborhood and subsequently averaged within a 500 m moving window. The local hypsometric integral (HI) was calculated using an elevation–relief approximation following Pike and Wilson [21]. Within a 1 km moving window, HI was expressed as:

$$HI = (\bar{z} - z_{min}) / (z_{maks} - z_{min}) \quad \ldots (2)$$

where $\bar{z}$ represents mean elevation and z_{min} and z_{max} are the minimum and maximum elevations within the corresponding neighborhood. The resulting index describes the relative position of mean elevation within local topographic relief.

Drainage density (Dd) was derived from a hydrologically conditioned DEM at 16 m resolution. Depressions were filled before drainage routing, and flow directions were determined using the D8 method [22]. Channel cells were identified using a contributing-area threshold of at least 0.05 km². Following the drainage-density concept introduced by Horton [23], local drainage density was calculated within a 1 km moving window as:

$$D_d = \Sigma L / A \quad \ldots (3)$$

where ΣL is the total length of the extracted channel segments within the neighborhood and A is the corresponding neighborhood area.

This drainage extraction procedure was applied consistently across the study area. However, flow routing over low-gradient surfaces may produce artificial drainage patterns, especially where the fixed contributing-area threshold does not adequately represent actual channel initiation conditions. The potential influence of this limitation was considered in the interpretation of the resulting terrain classes. Regional terrain position was represented using TPI, calculated as the difference between the elevation of a cell and the mean elevation of its surrounding neighborhood within a 2 km radius [24]. Positive values indicate relatively elevated terrain positions, whereas negative values indicate locations below the surrounding mean terrain elevation.

The moving-window sizes were selected to characterize terrain morphology at multiple spatial scales. The 500 m neighborhoods emphasized local terrain texture, the 1 km neighborhoods

represented broader relief and drainage characteristics, and the 2 km TPI neighborhood captured regional terrain position. The eight morphometric attributes and their respective calculation procedures are summarized in Table 1.

Table 1
Morphometric terrain attributes used for dem-based clustering

No	Morphometric attribute (unit)	Calculation method	Moving window	Geomorphological interpretation	Reference
1	Mean slope (°)	Mean slope derived using the Horn operator	500 m	Terrain steepness; resistant rocks may maintain steeper slopes	[18]
2	Slope standard deviation (°)	Standard deviation of slope gradient	500 m	Slope heterogeneity and variation in terrain dissection	[4]
3	Local relief (m)	Maximum minus minimum elevation	500 m	Local elevation amplitude and degree of terrain incision	[1]
4	Vector ruggedness measure (VRM) (dimensionless)	VRM calculated using Eq. (1), followed by spatial averaging	500 m	Three-dimensional terrain ruggedness, relatively independent of slope magnitude	[20]
5	Profile curvature variability (1/100 m)	Standard deviation of profile curvature	500 m	Frequency and variability of ridge–valley transitions	[19]
6	Drainage density (km/km²)	Total extracted D8 channel length per unit area; contributing area ≥0.05 km²	1 km	Terrain dissection and drainage network development	[23]
7	Local hypsometric integral (dimensionless)	Elevation–relief ratio calculated using Eq. (2)	1 km	Relative elevation distribution and landscape dissection characteristics	[21]
8	Regional topographic position index (TPI) (m)	Cell elevation minus mean elevation within a 2 km radius	2 km radius	Relative topographic position within the surrounding landscape	[24]

Table note: *All morphometric attributes were derived from DEMNAS elevation data at an 8 m grid resolution. VRM was initially calculated within a 5 × 5 pixel neighborhood before averaging over 500 m. Drainage density was derived from a hydrologically conditioned DEM at 16 m resolution. The eight attributes were subsequently aggregated to 120 m analysis cells, transformed where applicable, standardized, and subjected to principal component analysis before K-means clustering.*

2.4. *Spatial aggregation, feature transformation, and principal component analysis*

To reduce computational demands and characterize terrain properties at a consistent analytical scale, the eight morphometric rasters were aggregated from their original 8 m resolution to a 120 m analysis grid. Each analysis cell therefore represented a 15 × 15 pixel neighborhood of the original DEM grid. Attribute values were spatially averaged within each 120 m cell. Cells containing less than 80% valid pixels were excluded from subsequent analysis. This criterion also removed cells affected by incomplete moving-window support near the study-area boundary or the masked reservoir.

Following spatial aggregation and data screening, the analytical dataset contained 26,372 valid cells, representing approximately 379.8 km² of terrain. Each cell was represented by an eight-dimensional feature vector containing the selected morphometric attributes. Before dimensionality reduction, local relief, VRM, and profile curvature variability were subjected to logarithmic transformation to reduce positive skewness. All eight attributes were then standardized to z-scores using their respective means and standard deviations.

Standardization was performed to prevent attributes with larger numerical ranges or different physical units from dominating the Euclidean distances used in K-means clustering. Principal component analysis (PCA) was subsequently applied to the standardized feature matrix to reduce redundancy among correlated morphometric variables [7]. Components were retained until their cumulative explained variance reached at least 90% of the total feature variance.

The retained principal components served as the input features for K-means clustering. This procedure reduced the influence of strongly correlated original attributes on the distance-based classification while retaining most of the overall variance represented in the morphometric dataset. The PCA transformation was applied without incorporating geological labels. Consequently, the reduced feature space represented variations in terrain morphology rather than a supervised optimization of correspondence with the geological reference map.

2.5. *K-means clustering and determination of cluster number*

Unsupervised terrain classification was performed using the K-means clustering algorithm applied to the PCA-transformed morphometric dataset. K-means partitions observations into a predefined number of groups by minimizing the within-cluster sum of squared Euclidean distances [6]. The clustering objective function was expressed as:

$$J = \Sigma_j \Sigma_{i \in Cj} \|x_i - \mu_j\|^2 \quad \ldots (4)$$

where x_i represents the PCA-transformed feature vector of observation i, μ_j is the centroid of cluster j, and C_j denotes the set of observations assigned to that cluster.

Initial centroids were selected using the K-means++ initialization procedure [25] to reduce sensitivity to unfavorable initial centroid placement. The reference clustering solution was obtained using 50 independent initializations, and the solution minimizing within-cluster inertia was retained. Candidate cluster numbers ranging from $k = 2$ to $k = 10$ were evaluated using three complementary criteria: within-cluster inertia, the silhouette coefficient, and the Davies–Bouldin index.

The elbow point of the inertia curve was identified using the Kneedle algorithm [26]. This criterion was predefined as the principal basis for selecting the final number of clusters. Silhouette and Davies–Bouldin indices were calculated as complementary measures of internal clustering quality rather than as independent criteria that automatically determined the final classification. The silhouette coefficient measures the similarity of an observation to its assigned cluster relative to neighboring clusters [8]. For observation i, it was calculated as:

$$s(i) = [b(i) - a(i)] / maks\{a(i), b(i)\} \quad \ldots (5)$$

where $a(i)$ is the mean distance between observation i and other observations in the same cluster, and $b(i)$ is the lowest mean distance from observation i to observations in another cluster.

The Davies–Bouldin index was used to evaluate the relationship between within-cluster dispersion and separation between cluster centroids [9]. Lower values indicate relatively more compact and better-separated clusters according to this criterion. The final clustering solution was selected according to the predefined elbow criterion, while differences among the internal validation metrics were retained for interpretation. The cluster labels were subsequently ordered according to their mean slope values, with K1 assigned to the cluster exhibiting the highest mean slope. This label-ordering procedure facilitated consistent comparison of cluster characteristics without imposing geological classifications on the original unsupervised analysis.

2.6. *Clustering stability and spatial bootstrap assessment*

Clustering reproducibility was evaluated using adjusted Rand index (ARI), which measures the similarity between two partitions while correcting for agreement expected by chance [27].

Three complementary stability assessments were conducted to examine the sensitivity of the classification to initialization and data resampling. First, initialization stability was assessed using 30 additional K-means solutions generated with single initializations. The resulting partitions were compared with the reference solution to quantify the influence of centroid initialization on the final classification.

Second, conventional bootstrap stability was evaluated using 50 bootstrap samples of individual analysis cells. This procedure examined the sensitivity of the classification to changes in the sampled observations while treating cells as individual sampling units. Third, spatial dependence was considered using 50 spatial block bootstrap samples based on 2 × 2 km blocks. The purpose of spatial block resampling was to examine whether classification stability decreased when neighboring observations were resampled together rather than independently. This evaluation was motivated by the spatial autocorrelation inherent in gridded terrain datasets and by the importance of considering spatial structure when evaluating geographically dependent models [10].

For each stability assessment, partition similarity was summarized using ARI relative to the reference solution. The comparison between conventional and spatial block bootstrap results provided an indication of the extent to which spatial dependence influenced the apparent reproducibility of the clustering. High ARI values were interpreted as evidence of numerical partition stability rather than geological classification accuracy. Geological correspondence was evaluated separately using the reference geological map [3, 6, 16].

2.7. Geological correspondence and morphometric separability

The geological relevance of the resulting clusters was evaluated by comparing cluster assignments with lithological labels derived from the regional geological map [16]. Four complementary measures were used: normalized mutual information (NMI), adjusted Rand index (ARI), weighted cluster purity, and Cramér's V. NMI measures shared information between two classifications while accounting for differences in their entropy [28]. ARI evaluates agreement between pairs of observations assigned to the same or different groups [27]. Weighted purity describes the extent to which each terrain cluster is dominated by individual geological formations. Cramér's V was used to quantify the strength of association between morphometric cluster assignments and mapped geological formations. It was calculated as:

$$V = \sqrt{\{\chi^2 / [N\,(\min(r, c) - 1)]\}} \qquad \ldots (6)$$

where χ^2 is the chi-square statistic derived from the cluster–geology contingency table, N is the number of observations, and r and c represent the numbers of terrain clusters and geological categories, respectively.

These indices were used as complementary indicators because each measures a different aspect of correspondence between the unsupervised terrain classification and the geological reference dataset. To determine whether multivariate morphometric information improved geological discrimination, the reference classification was compared with two simpler alternatives: K-means clustering using mean slope alone and K-means clustering using local relief alone. Both single-attribute classifications were evaluated using the same number of clusters as the reference multivariate solution.

The resulting classifications were compared in terms of partition similarity and external geological agreement. This comparison provided a direct test of whether the integration of eight terrain attributes produced stronger geological correspondence than individual topographic descriptors. Because regional geological maps contain generalized formation boundaries, a second evaluation was performed using only interior cells located at least 300 m from mapped formation boundaries. This procedure reduced the influence of cells situated close to uncertain geological contacts, although it did not eliminate all uncertainty associated with the reference map.

Classification sensitivity was also evaluated for cluster numbers ranging from $k = 3$ to $k = 8$ and for reduced attribute combinations. In particular, the effects of excluding regional TPI, local hypsometric integral, and drainage density were examined to assess the influence of selected morphometric descriptors on geological correspondence.

The separability of individual geological formations was further investigated using Cliff's delta (δ), a nonparametric effect-size measure describing the degree of stochastic dominance between two distributions [29]. For two geological formations with attribute values x and y, Cliff's delta was expressed as:

$$\delta = [N(x_i > y_j) - N(x_i < y_j)] / (n_1\, n_2) \qquad \ldots (7)$$

where n1 and n2 represent the numbers of observations belonging to the two geological formations.

The absolute magnitude of δ was interpreted using the thresholds described by Romano et al. [30], with values below 0.147 considered negligible, values from 0.147 to below 0.33 considered small, values from 0.33 to below 0.474 considered medium, and values of at least 0.474 considered large. Particular attention was given to the comparison between mapped andesitic intrusions (a1) and the Kebobutak Formation (Tomk), which together represent a substantial proportion of the study area. Additional comparisons were performed for the Jonggrangan Formation, Sentolo Formation, and alluvial units to evaluate whether terrain attributes exhibited stronger discriminatory capacity for lithologies with contrasting geomorphological expressions.

The analysis was designed to evaluate morphometric separability rather than to infer mineralogical composition, rock strength, or subsurface geometry directly. Therefore, agreement with mapped lithological units was treated as external evidence of terrain–geology association rather than proof of geological equivalence.

2.8. Analytical workflow and interpretation framework

The complete analytical procedure is summarized in Fig. 2. The workflow consisted of DEM and geological data preparation, terrain attribute extraction, spatial aggregation, transformation and PCA, unsupervised K-means classification, cluster stability testing, and external geological evaluation. The analytical design intentionally separated three related but distinct evaluation dimensions [14, 22, 23].

First, internal clustering quality was assessed using inertia, silhouette, and Davies–Bouldin indices to characterize separation and compactness within the morphometric feature space. Second, numerical reproducibility was evaluated through repeated initialization, conventional bootstrap, and spatial block bootstrap experiments. These procedures examined the sensitivity of the resulting partitions to initialization and resampling conditions. Third, geological correspondence was evaluated through comparison with mapped formations, single-attribute classification benchmarks, boundary-interior analyses, sensitivity tests, and Cliff's delta comparisons [19–21].

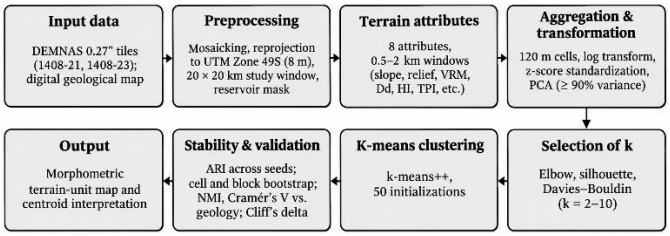


Fig. 2. Analytical workflow for DEMNAS-based morphometric terrain classification and geological evaluation, including DEM preprocessing, extraction of eight terrain attributes, spatial aggregation, feature transformation, PCA, K-means clustering, stability assessment, and comparison with regional geological units.

This framework enabled the study to evaluate whether multivariate terrain attributes improved geomorphological differentiation and geological correspondence independently, while identifying methodological limitations associated with interpreting stable terrain clusters as lithological units.

The separation was necessary because a classification may be statistically stable without accurately delineating lithological boundaries. Conversely, differences in geomorphological organization may be meaningful even when they do not coincide with individual geological formations. Accordingly, the resulting clusters were interpreted primarily as morphometric terrain domains. Their geological significance was assessed from observed associations with mapped formations rather than assumed from the clustering procedure itself [3, 6, 16].

3. Results and discussion

3.1. Spatial variability of DEM-derived morphometric attributes

The morphometric analysis was conducted using 26,372 valid terrain cells at a spatial resolution of 120 m, representing approximately 379.8 km² of the 400 km² study window. The excluded area consisted of the masked reservoir, peripheral cells with incomplete neighborhood support, and cells that did not satisfy the minimum valid-data requirement. The resulting analytical dataset provided continuous spatial coverage of the principal volcanic uplands, dissected slopes, transitional hills, and surrounding low-relief terrain of the central and southern Kulon Progo Mountains.

The eight DEM-derived terrain attributes exhibited substantial spatial variability, reflecting differences in terrain steepness, surface complexity, relative elevation, and drainage organization (Fig. 3). Mean slope and local relief showed their highest values within the central and northern mountainous terrain, where closely spaced ridges and deeply incised valleys produced substantial local elevation contrasts. In contrast, the western, eastern, and southern peripheral areas were characterized by relatively low slope gradients and reduced topographic relief.

Slope variability and the vector ruggedness measure (VRM) also highlighted the dissected volcanic terrain, particularly where steep valley flanks intersected with irregular ridge systems. These variables represented different aspects of terrain heterogeneity: slope standard deviation characterized the local variability of surface gradients, whereas VRM described changes in the orientation of surface-normal vectors. Their spatial distributions provided additional information about terrain complexity beyond mean slope alone.

Profile curvature variability further emphasized areas characterized by frequent transitions between convex ridges and concave valley surfaces. Higher curvature variability occurred within strongly dissected mountainous sectors, while lower values were generally associated with smoother surfaces and surrounding low-relief terrain. These patterns were consistent with the expectation that terrain dissection produces increased local morphological heterogeneity, although the resulting values may also be influenced by DEM smoothing, vegetation-related surface effects, and the selected moving-window scale.

Regional topographic position index (TPI) revealed a pronounced spatial organization of elevated ridges and incised valleys. Positive TPI values were associated with terrain positioned above the surrounding regional surface, whereas negative values corresponded to valleys and relatively depressed topographic positions. The contrast between positive and negative TPI values was particularly apparent within the central mountainous area, where ridge–valley networks radiated across the eroded volcanic landscape.

The local hypsometric integral exhibited relatively high values in the northern-central elevated terrain, including areas mapped as the Jonggrangan Formation. This pattern indicated differences in the distribution of elevation within local relief windows. However, local hypsometric values should not be interpreted directly as chronological erosion stages because they are influenced by terrain geometry, window size, lithological properties, and local landscape processes.

Drainage density displayed a more complex spatial pattern than the other attributes. Although elevated values were expected in dissected terrain, relatively high drainage-density values also occurred in low-gradient peripheral areas. This behavior suggested that the channel extraction procedure, based on a fixed contributing-area threshold and D8 flow routing, could generate artificial drainage networks on nearly flat terrain. Consequently, the drainage-density attribute required cautious interpretation when evaluating its geomorphological contribution to the classification.

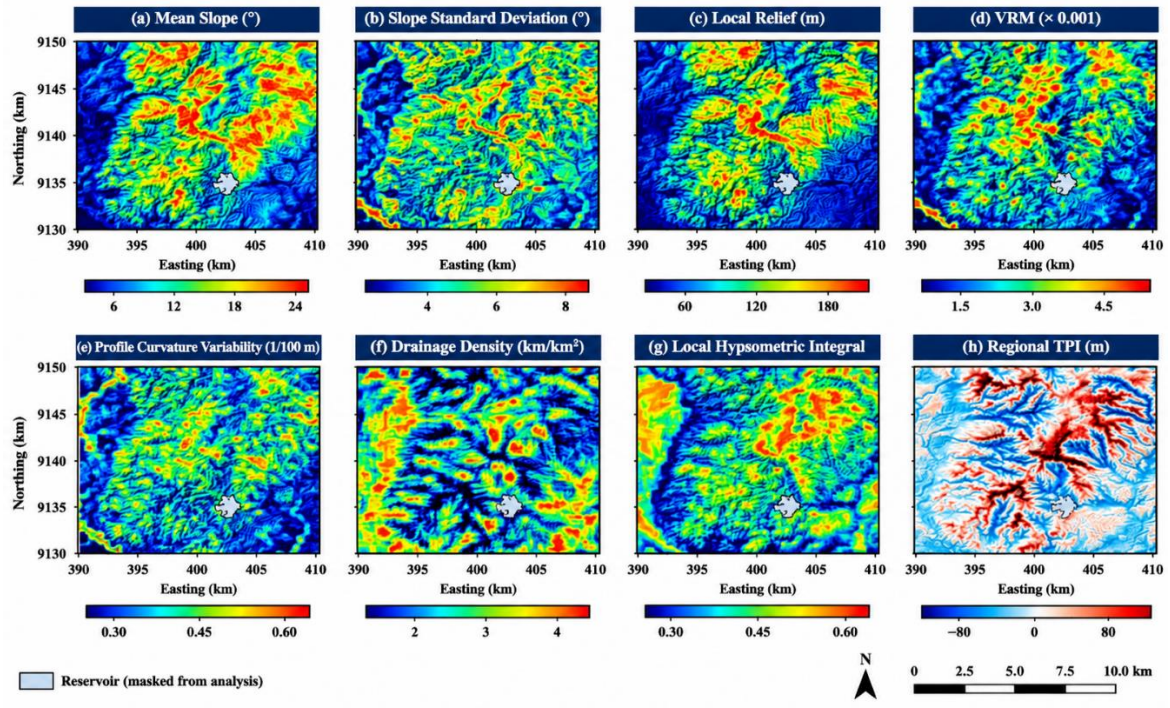


Fig 3. Spatial distribution of the eight DEMNAS-derived morphometric attributes aggregated to 120 m analysis cells and displayed over the shaded relief of the Kulon Progo Mountains: (a) mean slope, (b) slope standard deviation, (c) local relief, (d) vector ruggedness measure, (e) profile curvature variability, (f) drainage density, (g) local hypsometric integral, and (h) regional topographic position index. The maps illustrate spatial variations in terrain steepness, roughness, dissection, and relative topographic position.

The morphometric variables were not statistically independent. The strongest reported correlation occurred between mean slope and local relief (r = 0.94), demonstrating that these attributes captured strongly overlapping components of terrain morphology. Such correlation can influence Euclidean distance-based clustering by effectively assigning greater weight to closely related terrain properties when the original variables are used without dimensionality reduction.

Principal component analysis (PCA) was therefore applied to the standardized morphometric dataset. Four principal components were retained, explaining a cumulative 91.5% of the original attribute variance. The individual contributions of the retained components were 55.3%, 20.4%, 9.9%, and 5.9%, respectively. The dominance of the first principal component indicated that a substantial proportion of the multivariate terrain variation could be represented along a common direction in feature space. However, without the component-loading matrix, the relative contribution of individual terrain attributes to each principal component cannot be established directly. The interpretation of PCA components in terms of specific geomorphological processes therefore requires additional evaluation of their loadings.

Overall, the eight terrain attributes captured complementary aspects of the landscape but also exhibited substantial redundancy. These results provided the basis for examining whether the resulting multivariate feature space could distinguish geomorphological domains more effectively than individual terrain descriptors.

3.2. *Selection of the optimal number of terrain clusters*

The number of terrain clusters was evaluated for k = 2–10 using within-cluster inertia, the silhouette coefficient, and the Davies–Bouldin index (Fig. 4). These criteria provided complementary information about the structure of the morphometric feature space and the trade-off between classification simplicity and terrain differentiation. The lowest Davies–Bouldin index (0.959) and highest silhouette coefficient (0.400) were obtained at k = 2. This solution produced the strongest internal separation according to the two indices, primarily distinguishing the mountainous terrain from the surrounding low-relief areas.

Although the two-cluster solution represented a clear first-order geomorphological contrast, it did not provide sufficient differentiation of the internal terrain structure of the eroded volcanic complex. In particular, it combined topographically distinct mountainous domains that differed in relative terrain position and the degree of landscape dissection. For solutions containing at least three clusters, the highest silhouette coefficient occurred at k = 3 (0.309). However, the elbow criterion applied to the within-cluster inertia curve identified k = 4 as the preferred partition.

The four-cluster solution had a mean silhouette coefficient of 0.274 and a Davies–Bouldin index of 1.240. These values were less favorable than those obtained for the simpler two-cluster classification, indicating that the additional classes introduced greater overlap in multivariate feature space. The distribution of individual silhouette values further demonstrated the limited separation between some terrain clusters. Only 0.6% of cells exhibited negative silhouette coefficients, whereas only 5.4% had silhouette values greater than 0.5. This combination indicates that most cells were assigned without strongly negative silhouette values, but relatively few were strongly separated from neighboring clusters.

These results suggest that morphometric variability in the Kulon Progo landscape is characterized by gradual transitions rather than sharply separated terrain populations. Such continuity is consistent with the spatial organization of eroded volcanic terrain, where ridge positions, valley incision, and transitional slopes change progressively across the landscape.

The adoption of k = 4 should therefore be interpreted as a classification decision that provides additional geomorphological differentiation beyond the simpler mountainous–lowland partition. It should not be interpreted as evidence that four is the uniquely optimal number of natural terrain classes.

This distinction is important because internal clustering criteria measure statistical properties of the selected feature space rather than the geological validity of the resulting classes. A solution with a higher silhouette coefficient may provide a simpler statistical partition, while a solution with more clusters may reveal additional geomorphological organization at the expense of reduced separation. The four-cluster solution was retained for subsequent characterization, stability assessment, and geological comparison because it corresponded to the predefined elbow-selection procedure. The consequences of this choice were further examined through comparisons with alternative cluster numbers and single-attribute classifications.

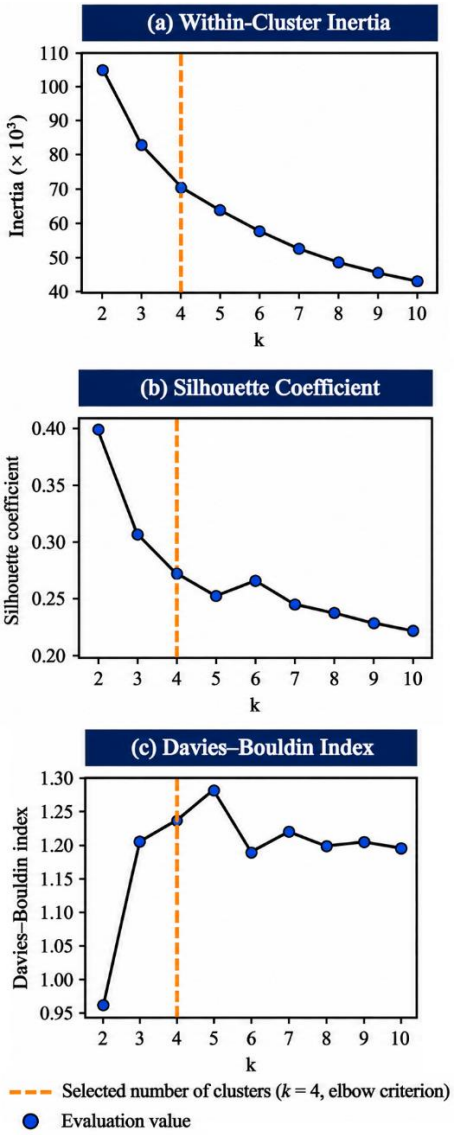


Fig. 4. Evaluation of candidate cluster numbers (k = 2–10) using (a) within-cluster inertia, (b) the silhouette coefficient, and (c) the Davies–Bouldin index. The dashed line indicates the selected four-cluster solution based on the elbow criterion. The silhouette and Davies–Bouldin indices favor simpler partitions, highlighting the trade-off between internal separation and geomorphological differentiation.

3.3. *Morphometric characteristics and spatial organization of terrain clusters*

The four-cluster solution delineated distinct terrain domains across the central and southern Kulon Progo Mountains (Fig. 5). The clusters differed in their slope characteristics, local relief, drainage density, hypsometric properties, and regional topographic position. Their spatial arrangement reflected differences in landscape morphology rather than a direct reproduction of geological formation boundaries. Cluster K1

occupied approximately 99.4 km², corresponding to 26.2% of the analyzed terrain. It was characterized by a median elevation of 428 m, mean slope of 19.6°, and local relief of 161 m. Its regional TPI was strongly positive (+73 m), indicating that the cluster predominantly occupied elevated positions relative to the surrounding landscape.

K1 also exhibited relatively low drainage density (1.99 km/km²) and a local hypsometric integral of 0.52. Its terrain characteristics were interpreted as representing elevated ridges and relatively weakly dissected upper surfaces within the volcanic complex. This interpretation describes the current morphology and does not independently establish the chronological age or original volcanic constructional surface of the terrain. The geological composition of K1 was dominated by the Kebobutak Formation (approximately 54%) and andesitic intrusions (33%), with the Jonggrangan Formation accounting for approximately 11%. Although the Jonggrangan Formation represented only a minor proportion of the cluster itself, approximately 55.4% of all cells mapped as Jonggrangan occurred within K1. This concentration was consistent with the elevated terrain characteristics of the Jonggrangan plateau.

Cluster K2 covered approximately 96.1 km², representing 25.3% of the analysis area. Its mean slope was 19.4°, closely comparable to that of K1, while local relief reached 148 m. Despite these similarities in terrain steepness, K2 differed substantially in regional topographic position, drainage organization, and terrain texture. Its regional TPI was strongly negative (−41 m), while drainage density reached 3.12 km/km² and the local hypsometric integral decreased to 0.44. These characteristics indicated that K2 predominantly represented incised valley flanks and highly dissected terrain positioned below the surrounding ridge network. The distinction between K1 and K2 is particularly important because their mean slopes differed by only 0.2°. Thus, the separation between these clusters could not be explained by mean slope alone. Instead, differences in topographic position, local terrain texture, and drainage organization contributed to the partition.

The standardized centroid profiles (Fig. 6) demonstrated contrasting morphometric characteristics between K1 and K2. K1 exhibited relatively high positive standardized values for mean slope, local relief, and regional TPI, whereas K2 showed stronger positive values for terrain ruggedness, curvature variability, and drainage density. These patterns indicate that multivariate morphometric classification can distinguish landscape positions and degrees of terrain dissection that are not adequately represented by slope magnitude alone.

However, the geological composition of K2 remained similar to that of K1. The Kebobutak Formation accounted for approximately 51% of K2, while andesitic intrusions contributed approximately 38%. This similarity suggests that K1–K2 separation primarily reflects internal geomorphological differentiation within a broadly comparable volcanic rock assemblage rather than the delineation of contrasting lithological units. Cluster K3 occupied approximately 100.2 km², representing 26.4% of the analyzed area. It had a median elevation of 124 m, mean slope of 12.5°, and local relief of 90 m. Its regional TPI was slightly negative (−13 m), and drainage density reached approximately 3.10 km/km².

Compared with K1 and K2, K3 represented terrain with intermediate slope gradients, reduced relief, and a more heterogeneous geological composition. The Kebobutak Formation accounted for approximately 38% of its area, followed by andesitic intrusions (29%) and alluvium (18%). The spatial distribution and morphometric characteristics of K3 were consistent with transitional footslopes and peripheral hills situated between the strongly dissected volcanic uplands and surrounding low-relief surfaces.

The heterogeneous geological composition of K3 emphasizes the transitional nature of this terrain domain. Its boundaries reflected gradual changes in terrain properties across the landscape, rather than sharp lithological contacts. Cluster K4 covered approximately 84.1 km², representing 22.2% of the analyzed terrain. It was the lowest-relief cluster, with a median elevation of 42 m, mean slope of 5.8°, and local relief of 31 m. The cluster was primarily composed of Quaternary alluvium (approximately 71%) and the Sentolo Formation (21%), corresponding to a terrain domain characterized by alluvial plains and low-relief sedimentary hills.

Approximately 70.5% of all mapped alluvial cells and 68.3% of Sentolo Formation cells occurred within K4. These proportions indicate that K4 was associated with the principal low-relief geological units, although it did not uniquely correspond to either formation. Unexpectedly, K4 exhibited the highest drainage density of all four clusters, reaching 3.66 km/km². This result was inconsistent with a straightforward interpretation of drainage density as an indicator of erosional dissection because K4 represented the lowest-relief terrain.

The high drainage-density value was attributed in the original analysis to artificial drainage networks generated by D8 routing across low-gradient surfaces. This interpretation indicates a potential limitation of the drainage extraction procedure rather than evidence of exceptionally intense dissection in the alluvial plains. Taken together, the four clusters represented a spatial sequence of elevated ridges, incised valley flanks, transitional footslopes, and low-relief plains. Their differences provided a useful description of the morphological organization of the eroded volcanic landscape.

However, the clusters should be regarded as morphometric terrain domains rather than independently validated lithological units. Their geological associations varied, and the boundaries between morphometric classes did not consistently coincide with mapped formation contacts.

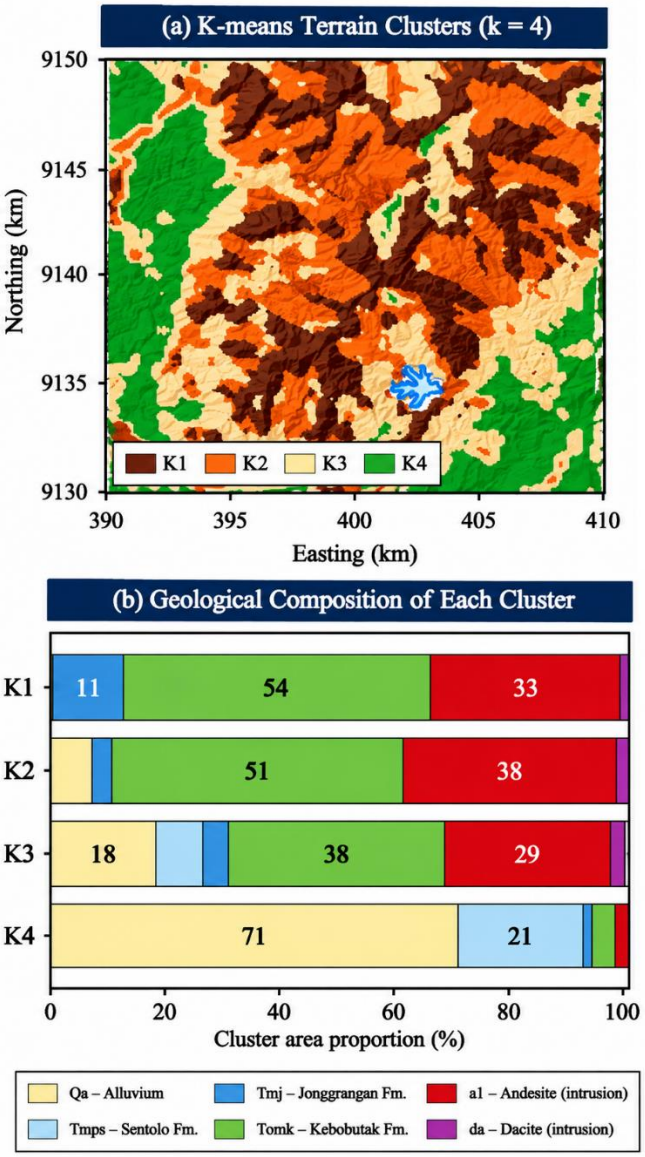


Fig. 5. Spatial and geological characteristics of the four K-means terrain clusters: (a) distribution of morphometric terrain domains across the Kulon Progo study area and (b) relative proportions of mapped geological formations within each cluster. The results show that the terrain clusters partially correspond to broad geological groups but do not consistently delineate individual volcanic and intrusive units.

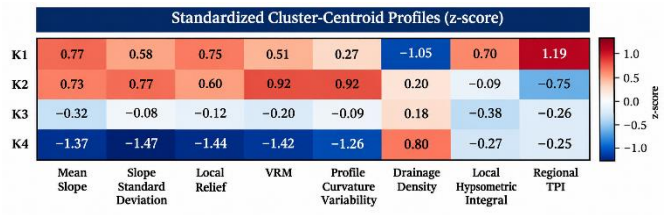


Fig. 6. Standardized morphometric centroid profiles of the four terrain clusters (K1–K4). Values represent standardized attribute characteristics used to distinguish the clusters. Contrasts between K1 and K2 emphasize the contribution of terrain position, ruggedness, curvature variability, and drainage organization to the differentiation of dissected volcanic terrain.

3.4. Reproducibility of morphometric terrain classification

The stability assessment demonstrated that the selected four-cluster partition was relatively reproducible under repeated initialization and data resampling (Table 2). Nevertheless, the degree of agreement depended on the evaluation procedure, particularly whether spatial dependence was considered. Across 30 additional single-initialization solutions, the adjusted Rand index (ARI) relative to the reference classification averaged 0.947 ± 0.114. The relatively high mean indicated that most initializations recovered similar terrain partitions, while the comparatively large standard deviation demonstrated that some individual solutions deviated substantially from the reference result.

This variability was interpreted as evidence that certain initializations converged to less favorable local minima of the K-means objective function. Accordingly, the reference solution was obtained using 50 initializations, reducing reliance on an individual centroid configuration. The conventional cell-based bootstrap produced an average ARI of 0.968 ± 0.013 across 50 resampling experiments. This result indicated high partition similarity under random resampling of individual terrain cells.

However, the spatial block bootstrap produced a lower average ARI of 0.878 ± 0.063. This reduction demonstrates that the apparent reproducibility of the classification was sensitive to the spatial structure of the sampled terrain observations. The difference between conventional and spatial block resampling is relevant because neighboring DEM cells are not independent observations. Spatial proximity often implies similar slope gradients, topographic positions, and local terrain textures. Randomly resampling individual cells may therefore retain much of the spatially redundant information present in the original dataset.

Table 2
Morphometric Characteristics and Geological Associations of the Four Terrain Clusters.

Cluster	Area (km²)	Area (%)	Median elevation (m)	Mean slope (°)	Local relief (m)	Drainage density (km/km²)	HI	TPI (m)
K1	99.4	26.2	428	19.6	161	1.99	0.52	+73
K2	96.1	25.3	274	19.4	148	3.12	0.44	−41
K3	100.2	26.4	124	12.5	90	3.10	0.41	−13
K4	84.1	22.2	42	5.8	31	3.66	0.43	−12

Cluster	Dominant geological formations (%)	Geomorphological interpretation
K1	Tomk 54; a1 33; Tmj 11	Elevated ridges and relatively weakly dissected upper surfaces
K2	Tomk 51; a1 38	Deeply incised valley flanks
K3	Tomk 38; a1 29; Qa 18	Transitional footslopes and peripheral hills
K4	Qa 71; Tmps 21	Alluvial plains and low-relief Sentolo hills

Note: *HI = local hypsometric integral; TPI = regional topographic position index; Tomk = Kebobutak Formation; a1 = andesite intrusion; Tmj = Jonggrangan Formation; Tmps = Sentolo Formation; Qa = Quaternary alluvium. Percentages of geological formations describe composition within each cluster. Values are rounded as reported in the original manuscript.*

Spatial block resampling changes the representation of different landscape sectors and provides a more demanding evaluation of partition consistency. The lower block-bootstrap ARI is consistent with greater sensitivity to the spatial distribution of terrain characteristics than suggested by conventional cell-based resampling. The spatial block results should nevertheless be interpreted as an assessment of reproducibility under the implemented resampling procedure, not as a complete quantification of spatial uncertainty. Their interpretation also depends on the 2 × 2 km block size, the handling of repeated blocks, and the procedures used to compare resampled solutions with the reference classification.

Importantly, the relatively high ARI values did not demonstrate that the clusters corresponded to geological formations. ARI in these tests measured agreement between alternative terrain partitions, whereas geological validity required independent comparison with mapped lithological units. The stability results therefore establish that the selected morphometric partition was reproducible under the tested conditions, particularly when multiple K-means initializations were used. They do not establish that the resulting boundaries are geological contacts or that each cluster represents a distinct rock unit.

This distinction forms a central component of the study: a terrain classification can exhibit substantial numerical stability while retaining limited geological discrimination. The following sections evaluate this relationship using external geological agreement metrics and comparisons with simpler terrain classifications.

3.5. Geological correspondence: multivariate clustering versus single-attribute classification

The external evaluation revealed a substantial distinction between the statistical reproducibility of morphometric terrain clusters and their correspondence with mapped geological formations. Although the four-cluster solution was relatively stable under bootstrap resampling, its geological agreement was moderate and consistently lower than that of classifications derived from individual topographic attributes. For the eight-attribute reference classification, the normalized mutual information (NMI) was 0.235, adjusted Rand index (ARI) was 0.166, Cramér's V was 0.454, and weighted cluster purity was 52.6% (Table 3). These values indicated partial correspondence between the morphometric clusters and geological units but did not support direct equivalence between the two classifications.

The results differed from the expectation that integrating multiple terrain attributes would necessarily improve lithological discrimination. When clustering was performed using mean slope alone, NMI increased to 0.303, ARI to 0.235, and Cramér's V to 0.511. Weighted purity also increased to 56.4%. Local relief produced an even stronger association with the regional geological map. Relief-only clustering yielded an NMI of 0.332, ARI of 0.253, and Cramér's V of 0.551, with weighted purity of 55.3%.

These results demonstrate that the multivariate classification did not outperform the simpler single-attribute alternatives in reproducing the mapped geological partition. The difference was particularly clear for Cramér's V, which increased from 0.454 for the eight-attribute solution to 0.511 for mean slope and 0.551 for local relief. The corresponding increase in NMI and ARI supported the same general conclusion. Therefore, the lower geological agreement of the multivariate classification was not restricted to a single external evaluation metric.

This finding is important because the objectives of morphometric terrain classification and lithological discrimination are not necessarily identical. The integration of slope, relief, ruggedness, curvature, drainage density, hypsometric properties, and topographic position may reveal geomorphological differences that are meaningful for describing landscape organization but do not coincide with mapped lithological boundaries.

The distinction between K1 and K2 provides a clear example. Both clusters were dominated by the Kebobutak Formation and andesitic intrusions, yet they differed strongly in topographic position, drainage density, and terrain texture. Consequently, the multivariate algorithm separated geomorphological domains within similar mapped geological assemblages.

Such separation contributed to terrain differentiation while potentially reducing agreement with the geological map because individual geological formations were divided among several morphometric clusters.

In contrast, slope-only and relief-only classifications emphasized dominant topographic gradients that were more closely associated with the broad geological divisions represented in the regional map. This produced stronger external agreement, although it did not establish that slope or relief could accurately distinguish all individual formations. The difference between multivariate and single-attribute classifications was also reflected in their spatial partitions. The ARI between the multivariate reference solution and slope-only classification was 0.361, whereas the corresponding ARI for relief-only classification was 0.272. These relatively low values indicated that the multivariate approach generated substantially different terrain partitions from those based on individual topographic variables.

This divergence supports the interpretation that the additional attributes introduced information related to terrain organization beyond mean slope or relief alone. However, the available results do not establish how much of this additional information represented geomorphologically meaningful variation versus sensitivity to attribute scales or extraction artifacts. The external comparison was repeated using only cells located at least 300 m from mapped geological formation boundaries. This interior-cell analysis included 18,327 cells and was intended to reduce the influence of positional uncertainty and boundary generalization in the regional geological reference map.

All three classifications exhibited stronger geological agreement when boundary-adjacent cells were excluded. For the multivariate solution, Cramér's V increased from 0.454 to 0.494, while NMI increased from 0.235 to 0.295. The slope-only classification showed a corresponding increase in Cramér's V from 0.511 to 0.566, and the relief-only classification increased from 0.551 to 0.611. These improvements indicate that disagreement near geological contacts contributed to the reduced correspondence observed in the complete dataset. However, the relative ranking of the three methods remained unchanged, with relief-only clustering producing the highest geological agreement, followed by slope-only clustering and then the multivariate classification.

The results were also evaluated across alternative cluster numbers. For k = 3–8, the reported Cramér's V values ranged from 0.341 to 0.545 for the multivariate classifications and from 0.352 to 0.602 for the slope-only classifications. The original sensitivity analysis reported that the multivariate classifications did not outperform the slope-only approach across the examined cluster numbers. Furthermore, removing regional TPI, the local hypsometric integral, or drainage density from the multivariate feature set did not substantially improve geological correspondence. The resulting Cramér's V values ranged from approximately 0.447 to 0.459.

Table 3
Agreement between morphometric terrain classifications and regional geological units

Classification	NMI	ARI	Cramér's V	Weighted purity (%)	Interior NMI	Interior Cramér's V
Eight-attribute PCA–K-means	0.235	0.166	0.454	52.6	0.295	0.494
Mean slope only	0.303	0.235	0.511	56.4	0.403	0.566
Local relief only	0.332	0.253	0.551	55.3	0.433	0.611

Note: *All classifications used k = 4. Interior statistics were calculated from 18,327 cells at least 300 m from mapped geological formation boundaries. NMI = normalized mutual information; ARI = adjusted Rand index. Larger values indicate stronger agreement with the reference geological partition, not necessarily greater geological truth or predictive accuracy.*

These results suggest that the reduced geological agreement was not attributable exclusively to one of these additional attributes. Instead, the difference between multivariate and single-attribute classifications likely reflects the broader effect of incorporating terrain characteristics that emphasize within-formation geomorphological variability. Nevertheless, the precise contribution of correlated attributes, PCA transformation, and processing scale to the reduced geological correspondence cannot be isolated using the reported results alone.

A further methodological consideration is the use of the regional geological map as an external reference. The reference map was prepared at a scale of 1:100,000 and therefore represents generalized lithological boundaries. Its geological categories may also contain substantial internal heterogeneity, especially in volcanic formations consisting of different rock types and emplacement products. Consequently, lower agreement with the geological map should not be interpreted automatically as poorer geomorphological classification. Rather, it indicates that the spatial organization represented by the morphometric clusters differs from the reference geological partition.

The combined results demonstrate that increasing the complexity of terrain descriptors can improve the differentiation of geomorphological domains without improving lithological correspondence. This distinction represents a central finding of the study and emphasizes the need to evaluate terrain classifications against objectives appropriate to their intended geological or geomorphological application.

3.6. Morphometric separability of volcanic and intrusive rock units

The comparison of individual morphometric attributes among geological formations provided additional evidence that terrain morphology did not consistently distinguish the mapped volcanic and intrusive rock units of the Kulon Progo Mountains. The most significant limitation concerned the separation of andesitic intrusions (a1) from the Kebobutak Formation (Tomk). Together, these two units occupied approximately 63% of the study window and were distributed across several morphometric terrain clusters.

The geological composition analysis demonstrated that both formations were predominantly associated with K1, K2, and K3. Approximately 37.4%, 33.8%, and 26.3% of all Kebobutak cells occurred in K1, K2, and K3, respectively. The corresponding proportions of andesitic intrusion cells were approximately 32.8%, 36.2%, and 29.1%. This similar distribution indicates that the morphometric classification did not reproduce a clear spatial separation between the two mapped geological units. Instead, both formations exhibited comparable proportions across terrain domains representing elevated ridges, incised valley flanks, and transitional footslopes.

The limited discrimination was further supported by the Cliff's delta analysis (Table 4). For the comparison between andesitic intrusions and the Kebobutak Formation, the absolute effect sizes were no greater than 0.27 across all eight attributes in the complete dataset. Mean slope showed almost no difference between the two formations (δ = −0.05), while local relief also exhibited a negligible effect (δ = −0.06). VRM, drainage density, and the local hypsometric integral similarly produced small absolute differences.

Table 4
Cliff's Delta Effect Sizes for Pairwise Comparisons of Geological Formations

Geological comparison	Mean slope	Slope SD	Relief	VRM	Curvature SD	Drainage density	HI	TPI
a1 – Tomk	−0.05	−0.27	−0.06	0.05	−0.09	0.04	−0.07	−0.20
a1 – Tomk (interior ≥500 m)	−0.24	−0.41	−0.20	−0.06	−0.24	0.08	−0.15	−0.14
Tmj – Tomk	−0.42	0.03	−0.24	−0.32	−0.17	0.13	0.57	0.40
Tmps – Tomk	−0.94	−0.86	−0.96	−0.87	−0.74	0.42	−0.10	−0.17
Tmps – Qa	0.40	0.11	0.57	−0.16	−0.14	−0.34	0.05	0.29

Note: *Bold values denote large effects (|δ| ≥ 0.474). a1 = andesite intrusion; Tomk = Kebobutak Formation; Tmj = Jonggrangan Formation; Tmps = Sentolo Formation; Qa = Quaternary alluvium; SD = standard deviation. Values are preserved from the original manuscript. The sign of δ reflects the order of the compared formations.*

Slope variability showed the largest absolute effect among the complete-data attributes (δ = −0.27), but this remained below the threshold used to classify a medium effect. These findings suggest that the two mapped geological units exhibited strongly overlapping morphometric distributions at the spatial scales examined. To reduce possible mixing near generalized geological boundaries, the comparison was repeated using cells located at least 500 m within the corresponding geological polygons. The resulting effect sizes increased for some attributes but remained below the threshold for a large effect.

Slope standard deviation exhibited the largest absolute effect in the interior-cell comparison (δ = −0.41), while mean slope and local relief

showed values of −0.24 and −0.20, respectively. This result indicates that excluding boundary-adjacent cells revealed somewhat stronger differences in certain terrain characteristics, but these differences remained insufficient to establish clear morphometric discrimination between andesitic intrusions and the Kebobutak Formation. An additional observation was that several differences occurred in directions opposite to a simple expectation that intrusive rocks would consistently form more resistant or elevated terrain. Within the regional reference map, the andesitic intrusion cells were generally associated with slightly lower slope gradients and relatively lower topographic positions than the surrounding Kebobutak cells.

However, the present analysis cannot determine whether these patterns result from differences in rock strength, weathering processes, internal geological heterogeneity, structural controls, or uncertainty in geological boundary delineation.

The Kebobutak Formation contains volcanic rock assemblages that may share compositional and structural characteristics with mapped andesitic intrusive bodies. In a deeply weathered tropical environment, the geomorphological expressions of these rocks may therefore overlap. Nevertheless, such geological explanations remain hypotheses because the study did not include comparative rock-strength measurements, weathering profiles, geochemical characterization, or independent field verification.

The results were substantially different for geological formations with more contrasting terrain characteristics. The Sentolo Formation exhibited strong morphometric differentiation from the Kebobutak Formation. Cliff's delta values for mean slope, slope standard deviation, local relief, VRM, and profile curvature variability were −0.94, −0.86, −0.96, −0.87, and −0.74, respectively. These large effect sizes indicated that the Sentolo Formation occupied terrain with substantially different steepness, relief, and surface-texture characteristics from the volcanic uplands mapped as the Kebobutak Formation.

The strong contrast was consistent with the spatial distribution of the Sentolo Formation within the lower-relief peripheral landscape. However, it should not be interpreted as evidence that morphometric attributes uniquely identify the geological composition of individual cells. The comparison between the Sentolo Formation and Quaternary alluvium showed a more selective pattern. Local relief exhibited a large positive effect (δ = 0.57), whereas mean slope showed a medium effect (δ = 0.40). Other attributes, including drainage density and the local hypsometric integral, displayed comparatively smaller differences. These results indicate that some terrain descriptors could distinguish parts of the Sentolo hills from surrounding alluvial plains despite their frequent association within the same low-relief terrain cluster.

The Jonggrangan Formation also exhibited distinctive morphometric characteristics. Its comparison with the Kebobutak Formation produced a large effect for the local hypsometric integral (δ = 0.57), whereas the other individual attributes showed smaller or moderate effects. This finding was consistent with the association of the Jonggrangan Formation with elevated terrain surfaces. Nevertheless, its morphometric separation was attribute-dependent rather than uniformly strong across all descriptors. The variation in Cliff's delta among geological formation pairs demonstrates that the usefulness of terrain attributes for geological discrimination depends strongly on the type of lithological contrast and the resulting landscape expression.

Where geological units occupy markedly different topographic environments, morphometric attributes may provide useful discriminatory information. Conversely, where units share similar volcanic compositions, weathering characteristics, and geomorphological settings, even combinations of multiple attributes may provide limited separation. The findings therefore support a distinction between broad terrain–geology association and the delineation of specific geological bodies. Morphometric classification may assist in identifying low-relief sedimentary domains, elevated geological surfaces, and differentiated erosional terrain. However, the results do not support reliable mapping of individual andesitic intrusions within the surrounding volcanic formations using the selected DEM-derived attributes alone.

3.7. *Geomorphological interpretation, methodological limitations, and implications for geological mapping*

The combined results demonstrate that DEM-based morphometric clustering captured meaningful differences in terrain organization within the eroded Kulon Progo paleovolcanic landscape. The four identified clusters reflected variations in relative topographic position, local relief, terrain complexity, and landscape dissection. The distinction between elevated upper surfaces and incised valley flanks was particularly informative because these domains exhibited similar mean slopes but contrasting regional TPI, drainage characteristics, and surface textures.

Such differences indicate that multivariate terrain descriptors can reveal geomorphological patterns that are not adequately represented by mean slope alone. In deeply eroded volcanic landscapes, these patterns may provide useful information about the spatial organization of ridges, valleys, and transitional landforms. However, the relationship between terrain characteristics and erosional history should be interpreted cautiously. The presence of relatively weakly dissected upper surfaces and deeply incised valley slopes does not independently establish their relative chronological development or demonstrate the sequence of geomorphic processes that produced the observed landscape.

Establishing such relationships would require additional geological, geomorphological, or chronological evidence. Therefore, the terrain domains identified in this study are more appropriately interpreted in terms of present-day morphology and relative dissection rather than as directly dated stages of landscape evolution. A central methodological implication is that internal clustering performance, numerical reproducibility, and geological correspondence represent distinct properties of a terrain classification. The relatively high bootstrap ARI values demonstrated that the selected partition could be recovered consistently under the tested resampling procedures. However, the moderate external agreement with mapped geological formations indicated that this reproducibility did not correspond to equally strong lithological discrimination.

Furthermore, the lower agreement of the multivariate classification relative to slope-only and relief-only approaches demonstrated that increasing the number of terrain attributes may introduce geomorphological distinctions that do not align with geological formation boundaries.

This finding does not necessarily indicate that multivariate terrain analysis is ineffective. Instead, it emphasizes that the suitability of a classification depends on the intended application. A classification optimized for describing landscape organization may differ substantially from a classification designed to reproduce mapped geological units. Several methodological limitations should be considered when interpreting these results.

First, the selected attributes were derived from a single elevation dataset. Although DEMNAS provides relatively detailed terrain information, DEM-based derivatives may be influenced by elevation uncertainty, interpolation, vegetation-related surface effects, and the representation of the actual ground surface. These effects may be especially relevant in densely vegetated tropical areas, where the measured elevation surface may include contributions from vegetation or other aboveground features.

Second, terrain attributes were calculated using different neighborhood sizes. Local terrain texture was represented primarily through 500 m moving windows, drainage and hypsometric properties through 1 km windows, and regional terrain position through a 2 km radius. These scales influence the spatial structures emphasized by each attribute and may affect the resulting clusters. The original analysis examined the sensitivity of geological correspondence to certain attribute exclusions, but a systematic assessment of alternative moving-window sizes and aggregation resolutions was not reported. Therefore, the extent to which the observed terrain partitions depend on these spatial scales remains unresolved.

Third, the drainage-density calculation was sensitive to the extraction of artificial channel networks across low-gradient surfaces. The high drainage density associated with K4 demonstrated that the selected D8 routing and fixed contributing-area threshold did not always produce a straightforward indicator of terrain dissection. Because drainage density was included in the clustering feature set, this artifact could have influenced the position of observations in multivariate feature space. Although the reported attribute-removal

tests indicated limited changes in geological agreement, they did not establish that the spatial boundaries of individual clusters were unaffected.

Fourth, the geological reference dataset was derived from a regional map at a scale of 1:100,000. Geological boundaries at this scale are generalized, and mapped units may contain substantial internal variations in lithology, degree of weathering, structure, and geomorphic expression. The increased agreement observed for interior cells indicated that boundary uncertainty contributed to the overall mismatch. Nevertheless, the interior-cell analysis did not eliminate uncertainty arising from geological classification or within-formation heterogeneity.

Fifth, the analysis did not include independent outcrop verification, petrographic data, or geophysical measurements capable of directly testing the relationship between morphometric clusters and the distribution of individual intrusive bodies. Consequently, the present results should be interpreted as an evaluation of associations between terrain attributes and mapped geological units rather than an independently validated lithological classification.

The limited separability of andesitic intrusions and the Kebobutak Formation has important implications for geological mapping in eroded volcanic regions. Where intrusive and extrusive rocks exhibit similar surface morphologies, DEM-derived attributes alone may not provide sufficient information to delineate their boundaries. Complementary datasets could potentially address this limitation. Geological field observations, remote sensing information, and subsurface geophysical measurements may provide additional constraints on the distribution of lithological units.

Gravity data represent one possible complementary source because subsurface density variations can produce measurable gravity anomalies. However, successful discrimination of intrusive bodies would depend on the existence of sufficient density contrast relative to surrounding rocks, as well as body geometry, survey resolution, and the availability of independent geological constraints. Accordingly, gravity integration should be considered a testable direction for subsequent research rather than an established solution to the ambiguity observed in the present morphometric classification. Future studies could also evaluate alternative terrain classification procedures, spatial scales, and feature combinations. Such comparisons would help determine whether the limited lithological correspondence primarily reflects the selected K-means partition, the morphometric information contained in the elevation data, or the geological similarity of the mapped units.

Additional investigation should prioritize field verification across K1–K2 boundaries, improved drainage-network extraction using terrain-sensitive channel initiation criteria, and sensitivity analyses involving moving-window size and classification resolution. Ultimately, this study demonstrates that reproducible terrain classification and geological discrimination should be evaluated independently. DEM-based morphometric clustering provides a useful framework for characterizing geomorphological organization within deeply eroded volcanic landscapes, but stable clusters should not be interpreted automatically as geological formations or intrusive bodies. The broader implication is that terrain classification can contribute to geological investigation most effectively when its geomorphological information content is explicitly distinguished from independent evidence of lithological boundaries.

4. Conclusion

This study evaluated the ability of unsupervised DEM-based morphometric classification to characterize terrain organization and discriminate geological units within the deeply eroded paleovolcanic landscape of the Kulon Progo Mountains, Indonesia. Eight morphometric attributes derived from DEMNAS were integrated using principal component analysis and K-means clustering, resulting in four terrain domains representing relatively weakly dissected upper surfaces, incised valley flanks, transitional footslopes, and low-relief alluvial plains and Sentolo hills. The resulting classification exhibited high numerical reproducibility, with adjusted Rand indices of 0.968 for conventional cell-based bootstrapping and 0.878 for spatial block bootstrapping. However, geological correspondence remained limited. The multivariate classification produced a Cramér's V of 0.454, lower than the values obtained from slope-only (0.511) and relief-only (0.551) classifications. Furthermore, mapped andesitic intrusions and the Kebobutak Formation exhibited weak morphometric separability, with absolute Cliff's delta values not exceeding 0.27 across the evaluated attributes. These findings demonstrate that statistically reproducible terrain partitions do not necessarily correspond to distinct lithological units and that incorporating additional morphometric variables does not inherently improve geological discrimination.

The results highlight the importance of distinguishing geomorphological information from lithological interpretation when applying unsupervised terrain classification to eroded volcanic landscapes. Multivariate morphometric analysis provided useful differentiation of terrain position, surface complexity, and relative landscape dissection, but its capacity to delineate individual intrusive bodies was constrained by overlapping terrain characteristics and uncertainty in the regional geological reference map. The findings are also subject to limitations associated with DEM surface representation, scale-dependent terrain attributes, and drainage-network extraction artifacts. Future investigations should evaluate the sensitivity of terrain classifications to spatial resolution and moving-window size, incorporate independent geological field observations, and investigate complementary geophysical constraints, including gravity data where sufficient density contrasts exist. Overall, this study demonstrates that clustering stability and geological correspondence must be evaluated independently, providing a more rigorous basis for interpreting DEM-derived terrain classifications in deeply eroded volcanic environments.

CRediT authorship contribution statement

Rizqi Prastowo: Writing – original draft, Methodology, Investigation, Formal analysis, Data curation, Visualization. **Ignatius Adi Prabowo:** Validation, Methodology, Formal analysis, Writing – review & editing.

Declaration of Competing Interest

The authors declare that they have no known competing financial interests or personal relationships that could have appeared to influence the work reported in this paper.

Data availability

Data will be made available on request.

Acknowledgment

The authors gratefully acknowledge the Geospatial Information Agency of Indonesia (Badan Informasi Geospasial, BIG) for providing access to the Indonesian National Digital Elevation Model (DEMNAS), which served as the primary elevation dataset for the morphometric analysis. The authors also acknowledge the Geological Research and Development Centre, Geological Agency of Indonesia, for providing the digital geological map used as an independent reference for evaluating the correspondence between morphometric terrain clusters and mapped geological formations. These geospatial datasets provided the foundation for investigating terrain organization and the limitations of lithological discrimination in the deeply eroded paleovolcanic landscape of the Kulon Progo Mountains, Indonesia.

References

1. Grosse, P., van Wyk de Vries, B., Euillades, P. A., Kervyn, M., and Petrinovic, I. A. (2012). Systematic Morphometric Characterization of Volcanic Edifices Using Digital Elevation Models, Geomorphology, Vol. 136, No. 1, pp. 114–131. doi:10.1016/j.geomorph.2011.06.001.

2. Karátson, D., Telbisz, T., and Wörner, G. (2012). Erosion Rates and Erosion Patterns of Neogene to Quaternary Stratovolcanoes in the Western Cordillera of the Central Andes: An SRTM DEM Based Analysis, Geomorphology, Vol. 139–140, pp. 122–135. doi:10.1016/j.geomorph.2011.10.010.
3. Selby, M. J. (1980). A Rock Mass Strength Classification for Geomorphic Purposes: With Tests from Antarctica and New Zealand, Zeitschrift für Geomorphologie, Vol. 24, No. 1, pp. 31–51.
4. Iwahashi, J., and Pike, R. J. (2007). Automated Classifications of Topography from DEMs by an Unsupervised Nested-Means Algorithm and a Three-Part Geometric Signature, Geomorphology, Vol. 86, No. 3–4, pp. 409–440. doi:10.1016/j.geomorph.2006.09.012.
5. Iwahashi, J., Kamiya, I., Matsuoka, M., and Yamazaki, D. (2018). Global Terrain Classification Using 280 m DEMs: Segmentation, Clustering, and Reclassification, Progress in Earth and Planetary Science, Vol. 5, Article 1. doi:10.1186/s40645-017-0157-2.
6. Jain, A. K. (2010). Data Clustering: 50 Years Beyond K-Means, Pattern Recognition Letters, Vol. 31, No. 8, pp. 651–666. doi:10.1016/j.patrec.2009.09.011.
7. Jolliffe, I. T., and Cadima, J. (2016). Principal Component Analysis: A Review and Recent Developments, Philosophical Transactions of the Royal Society A, Vol. 374, No. 2065, Article 20150202. doi:10.1098/rsta.2015.0202.
8. Rousseeuw, P. J. (1987). Silhouettes: A Graphical Aid to the Interpretation and Validation of Cluster Analysis, Journal of Computational and Applied Mathematics, Vol. 20, pp. 53–65. doi:10.1016/0377-0427(87)90125-7.
9. Davies, D. L., and Bouldin, D. W. (1979). A Cluster Separation Measure, IEEE Transactions on Pattern Analysis and Machine Intelligence, Vol. PAMI-1, No. 2, pp. 224–227. doi:10.1109/TPAMI.1979.4766909.
10. Roberts, D. R., et al. (2017). Cross-Validation Strategies for Data with Temporal, Spatial, Hierarchical, or Phylogenetic Structure, Ecography, Vol. 40, No. 8, pp. 913–929. doi:10.1111/ecog.02881.
11. Grebby, S., Naden, J., Cunningham, D., and Tansey, K. (2011). Integrating Airborne Multispectral Imagery and Airborne LiDAR Data for Enhanced Lithological Mapping in Vegetated Terrain, Remote Sensing of Environment, Vol. 115, No. 1, pp. 214–226. doi:10.1016/j.rse.2010.08.019.
12. Julzarika, A., and Harintaka. (2019). Indonesian DEMNAS: DSM or DTM?, Proceedings of the 2nd IEEE Asia-Pacific Conference on Geoscience, Electronics and Remote Sensing Technology (AGERS), Jakarta, Indonesia, pp. 31–36. doi:10.1109/AGERS48446.2019.9034351.
13. van Bemmelen, R. W. (1949). The Geology of Indonesia, Vol. IA, Martinus Nijhoff, The Hague, Netherlands.
14. Syafri, I., Budiadi, E., and Sudradjat, A. (2013). Geotectonic Configuration of Kulon Progo Area, Yogyakarta, Indonesian Journal on Geoscience, Vol. 8, No. 4, pp. 185–190. doi:10.17014/ijog.8.4.185-190.
15. Rahardjo, W., Sukandarrumidi, and Rosidi, H. M. D. (1995). Peta Geologi Lembar Yogyakarta, Jawa, Scale 1:100,000, Pusat Penelitian dan Pengembangan Geologi, Bandung, Indonesia.
16. Pusat Penelitian dan Pengembangan Geologi. (2010). Peta Geologi Indonesia, Digital GIS Dataset (Geologi.shp), Badan Geologi, Bandung, Indonesia.
17. Pedregosa, F., et al. (2011). Scikit-Learn: Machine Learning in Python, Journal of Machine Learning Research, Vol. 12, pp. 2825–2830.
18. Horn, B. K. P. (1981). Hill Shading and the Reflectance Map, Proceedings of the IEEE, Vol. 69, No. 1, pp. 14–47. doi:10.1109/PROC.1981.11918.
19. Zevenbergen, L. W., and Thorne, C. R. (1987). Quantitative Analysis of Land Surface Topography, Earth Surface Processes and Landforms, Vol. 12, No. 1, pp. 47–56. doi:10.1002/esp.3290120107.
20. Sappington, J. M., Longshore, K. M., and Thompson, D. B. (2007). Quantifying Landscape Ruggedness for Animal Habitat Analysis: A Case Study Using Bighorn Sheep in the Mojave Desert, Journal of Wildlife Management, Vol. 71, No. 5, pp. 1419–1426. doi:10.2193/2005-723.
21. Pike, R. J., and Wilson, S. E. (1971). Elevation-Relief Ratio, Hypsometric Integral, and Geomorphic Area-Altitude Analysis, Geological Society of America Bulletin, Vol. 82, No. 4, pp. 1079–1083. doi:10.1130/0016-7606(1971)82[1079:ERHIAG]2.0.CO;2.
22. O'Callaghan, J. F., and Mark, D. M. (1984). The Extraction of Drainage Networks from Digital Elevation Data, Computer Vision, Graphics, and Image Processing, Vol. 28, No. 3, pp. 323–344. doi:10.1016/S0734-189X(84)80011-0.
23. Horton, R. E. (1945). Erosional Development of Streams and Their Drainage Basins: Hydrophysical Approach to Quantitative Morphology, Geological Society of America Bulletin, Vol. 56, No. 3, pp. 275–370. doi:10.1130/0016-7606(1945)56[275:EDOSAT]2.0.CO;2.
24. De Reu, J., et al. (2013). Application of the Topographic Position Index to Heterogeneous Landscapes, Geomorphology, Vol. 186, pp. 39–49. doi:10.1016/j.geomorph.2012.12.015.
25. Arthur, D., and Vassilvitskii, S. (2007). K-Means++: The Advantages of Careful Seeding, Proceedings of the 18th Annual ACM-SIAM Symposium on Discrete Algorithms (SODA), New Orleans, USA, pp. 1027–1035. doi:10.1145/1283383.1283494.
26. Satopää, V., Albrecht, J., Irwin, D., and Raghavan, B. (2011). Finding a "Kneedle" in a Haystack: Detecting Knee Points in System Behavior, Proceedings of the 31st International Conference on Distributed Computing Systems Workshops, Minneapolis, USA, pp. 166–171. doi:10.1109/ICDCSW.2011.20.
27. Hubert, L., and Arabie, P. (1985). Comparing Partitions, Journal of Classification, Vol. 2, pp. 193–218. doi:10.1007/BF01908075.
28. Vinh, N. X., Epps, J., and Bailey, J. (2010). Information Theoretic Measures for Clusterings Comparison: Variants, Properties, Normalization and Correction for Chance, Journal of Machine Learning Research, Vol. 11, pp. 2837–2854.
29. Cliff, N. (1993). Dominance Statistics: Ordinal Analyses to Answer Ordinal Questions, Psychological Bulletin, Vol. 114, No. 3, pp. 494–509. doi:10.1037/0033-2909.114.3.494.
30. Romano, J., Kromrey, J. D., Coraggio, J., and Skowronek, J. (2006). Appropriate Statistics for Ordinal Level Data: Should We Really Be Using t-Test and Cohen's d for Evaluating Group Differences on the NSSE and Other Surveys?, Annual Meeting of the Florida Association of Institutional Research, Cocoa Beach, USA..1.2020.31-41.